

Dynamic Behavior of Heterobimetallic Derivatives of Cycloheptatriene. Chemically Induced Switch of the Vibration Mode in Molecular Oscillators

Ilya D. Gridnev* and Mia Karenina C. del Rosario

COE Laboratory, Department of Chemistry, Graduate School of Science, Tohoku University, Aoba, Sendai, 980-8578, Japan

Received January 18, 2005

Two new heterobimetallic complexes, (7-*exo*-triphenylstannyl)- η^4 -cycloheptatrienyliirontricarboxyl (**3**) and (7-*exo*-triphenylstannyl)- η^4 -cycloheptatrienyli rutheniumtricarboxyl (**5**), have been synthesized via the ligand exchange reactions from triphenyl(cycloheptatrienyl)tin (**1**). Both **3** and **5** are fluxional. Facile [1,3]-Fe and [1,3]-Ru haptotropic shifts are the fastest dynamic processes observed in **3** and **5**, respectively. Slower diatropic rearrangements involving simultaneous [1,7]-Sn and [1,2]-M (or [1,4]-M) migrations (M = Fe, Ru) were observed in each case. Activation parameters of the fast rearrangements in **3** and **5** were determined via 2D EXSY NMR (^1H and ^{13}C). The mode of intramolecular oscillations was switched in solution by reacting **3** with bromodimethylborane, which yielded cleanly (7-*exo*-phenyl(methyl)boryl)- η^4 -cycloheptatrienyliirontricarboxyl (**14**), which exhibited a single type of intramolecular dynamics, viz., [1,7]-B + [1,2]-Fe diatropic rearrangement.

Introduction

Various types of intramolecular motion are now under intense attention of chemists in connection with the efforts aimed at the creation of molecular devices imitating the natural ATP-¹ or DNA-based² molecular machines. This goal provides tremendous challenges for the molecular design and synthesis of appropriate molecules, and as it has been recently pointed out, the realization of a truly operative molecular device (implying the necessity to overcome the stochastic behavior of molecular assemblies) is probably quite a remote prospect.³

Nevertheless, the concept itself is useful in stimulating chemists to undertake brave and beautiful synthetic projects. This situation is similar to the total synthesis of huge natural products, however is much more susceptible to frustration, since quite often the achieved synthetic goal does not possess the expected properties necessary for being a prototype of a molecular device.⁴ On the other hand, the research in the area of the potential molecular devices creates a more general and elaborate view on the molecular structure and, in particular, on the controlled intramolecular motion that is a driving force of any molecular machine.⁵ Thus, conformational rotation controlled either by clever

design of substituents around the rotating bond⁶ or by coordination of a certain part of the molecule with metallic templates⁷ has been widely used for the construction of molecular devices. Another approach is based on the photochemically assisted rotation around double bonds, whereas the direction of rotation can be controlled by proper design of substituents.⁸ Supramolecular devices usually apply reversible coordination of the sliding parts of the molecule to the metal ions via donor atoms.⁹ However, surprisingly, metallotropic rearrangements have not been so far analyzed as the possible source of a controlled intramolecular motion.

Although the fastest metallotropic migrations are comparable in their rates with conformational equilibria, unlike the latter they are strictly regulated electronically.¹⁰ The simple MO theory correctly predicts the modes of migration for different elements in the compounds with either σ - or π -bonded organometallic groups.^{10c} The mode and rate of rearrangement can be

(1) (a) Abrahams, J. P.; Leslie, A. G. W.; Lutter, R.; Walker, J. E. *Nature* **1994**, *370*, 621. (b) Noji, H.; Yasuda, R.; Yoshida, M.; Kinoshita, K., Jr. *Nature* **1997**, *386*, 299. (c) Rayment, I.; Holden, H. M.; Whittaker, M.; Yohn, C.; Lorenz, M.; Holmes, K. C.; Milligan, R. A. *Science* **1993**, *261*, 50.

(2) (a) Mao, C.; Sun, W.; Shen, Z.; Seeman, N. C. *Nature* **1999**, *397*, 144. (b) Yurke, B.; Turberfield, A. J.; Mills, A. P.; Simmel, F. C.; Neumann, J. L. *Nature* **2000**, *406*, 605. (c) Feng, L.; Park, S. H.; Reif, J. H.; Yan, H. *Angew. Chem., Int. Ed.* **2003**, *42*, 4342. (d) Chen, Y.; Mao, C. *J. Am. Chem. Soc.* **2004**, *126*, 8626.

(3) Easton, C. J.; Lincoln, S. E.; Barr, L.; Onagi, H. *Chem. Eur. J.* **2004**, *10*, 3120.

(4) Kelly, T. R. *Acc. Chem. Res.* **2001**, *34*, 514.

(5) Balzani, V.; Credi, A.; Venturi, M. *Chem. Eur. J.* **2002**, *8*, 5525.

(6) (a) Kelly, T. R.; Tellitu, I.; Sestelo, J. P. *Angew. Chem., Int. Ed. Engl.* **1997**, *36*, 1866. (b) Kelly, T. R.; Sestelo, J. P.; Tellitu, I. *J. Org. Chem.* **1998**, *63*, 3655. (c) Kelly, T. R.; De Silva, H.; Silva, R. A. *Nature* **1999**, *401*, 150. (d) Kelly, T. R.; Silva, R. A.; De Silva, H.; Jasmin, S.; Zhao, Y. A. *J. Am. Chem. Soc.* **2000**, *122*, 6935.

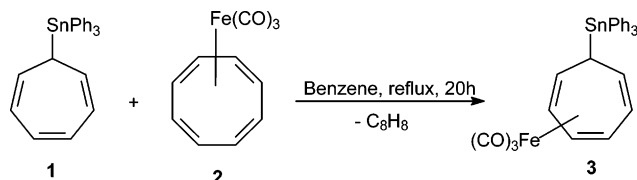
(7) Kelly, T. R.; Bowyer, M. C.; Bhaskar, K. V.; Bebbington, D.; Garcia, A.; Lang, F.; Kim, M. H.; Jette, M. P. *J. Am. Chem. Soc.* **1994**, *116*, 3657.

(8) (a) Feringa, B. L. *Acc. Chem. Res.* **2001**, *34*, 504. (b) Koumura, N.; Geertsema, E. M.; van Gelder, M. B.; Meetsma, A.; Feringa, B. L. *J. Am. Chem. Soc.* **2002**, *124*, 5037.

(9) Ashton, P. R.; Ballardini, R.; Balzani, V.; Credi, A.; Dress, K. R.; Ishow, E.; Kleverlaan, C. J.; Koichan, O.; Preece, J. A.; Spencer, N.; Stoddart, J. F.; Venturi, M.; Wenger, S. *Chem. Eur. J.* **2000**, *6*, 3558.

(10) (a) Woodward, R. B.; Hoffmann, R. *The Conservation of Orbital Symmetry*; Verlag Chemie: Weinheim, 1970. (b) Larrabee, R. B. *J. Am. Chem. Soc.* **1971**, *93*, 1510. (c) Gridnev, I. D.; Schreiner, P. R.; Tok, O. L.; Bubnov, Yu. N. *Chem. Eur. J.* **1999**, *5*, 2042. (d) Gridnev, I. D.; Tok, O. L. In *Fluxional Organometallic and Coordination Compounds*; Gielen, M., Willem, R., Wrackmeyer, B., Eds.; Wiley: The Atrium, 2004; pp 41–83.

Scheme 1



tuned by appropriate choice of the organometallic group. These features make the metallotropic rearrangements promising candidates for the prototypes of molecular motors. Cotton and Reich were first to demonstrate that both metals in heterobimetallic complexes can be involved in the synchronous intramolecular motion by the analysis of the temperature-dependent ^1H NMR spectra of the bimetallic $\mu\text{-}\eta^3\text{:}\eta^4\text{-Cp}(\text{CO})_2\text{Mo}(\text{C}_7\text{H}_7)\text{Fe}(\text{CO})_3$ complex.¹¹ They concluded that the most probable mechanism of the observed fluxionality is the simultaneous [1,2] shift of both metals with the probable admixture of the [1,3] shift mechanism.¹¹ Although quite a few dynamic heterobimetallic complexes were characterized afterward,¹² the topology of the observed rearrangements has been rarely probed, and the regulations governing the selectivity of such migrations are unknown so far. Recently, we have reported the cooperative effects on the character of the intramolecular dynamics in heterobimetallic complexes: introduction of the second organometallic group changes the mode of migration and can either facilitate¹³ or lock electronically¹⁴ the rearrangements occurring in an organometallic molecule. In this paper we report the synthesis of new heterobimetallic complexes and the experimental analysis of their dynamic behavior and demonstrate the possibility to switch chemically the mode of vibrations in two-centered molecular oscillators.

Results

Synthesis and Thermal Rearrangements of Irontricarboxyl and Rutheniumtricarboxyl Complexes of Triphenyl(cycloheptatrienyl)tin. Iron complex **3** was synthesized by the exchange reaction of triphenyl(cycloheptatrienyl)tin (**1**) with a 2-fold excess of tricarbonyl(cyclooctatetraene)iron (**2**) (Scheme 1). The target complex **3** is unstable in the air and yields quantitatively tricarbonyl(η^4 -cycloheptatrienyl)iron when passed through the column. Therefore, to get pure **3**, it was necessary to use a 2-fold excess of **2** to shift the equilibrium toward the formation of **3** and remove the

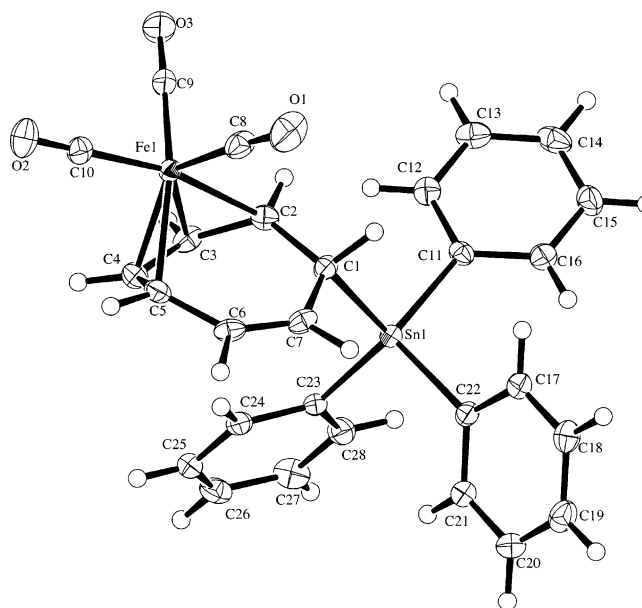
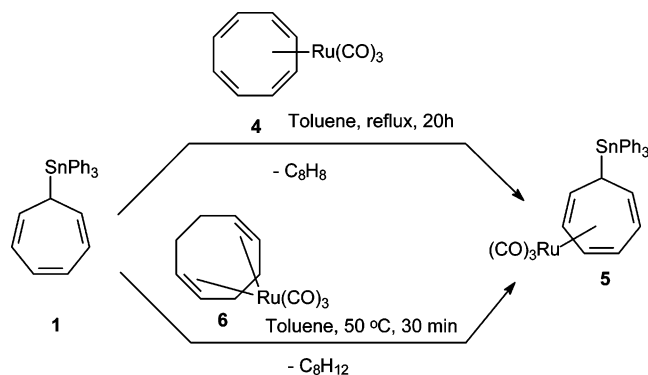


Figure 1. ORTEP diagram of complex **3** (50% thermal ellipsoids). Selected bond lengths (\AA): Sn(1)–C(1) 2.217(3), C(1)–C(7) 1.472(4), C(1)–C(2) 1.498(4), C(2)–C(3) 1.438(4), C(3)–C(4) 1.398(4), C(4)–C(5) 1.428(5), C(5)–C(6) 1.474(4), C(6)–C(7) 1.335(4), Fe(1)–C(2) 2.172(3), Fe(1)–C(3) 2.059(3), Fe(1)–C(4) 2.045(3), Fe(1)–C(5) 2.150(3).

Scheme 2



excess of **2** by sublimation after the reaction was complete. The structure of **3** has been established by a combination of spectral methods and confirmed by microanalysis and single-crystal X-ray structure (Figure 1).

Reaction of tricarbonyl(cyclooctatetraene)ruthenium (**4**) with **1** afforded the ruthenium complex **5** (Scheme 2), but the reaction required harder conditions that led to thermal rearrangements of **5** (vide supra). We have found that a more convenient access to **5** is the reaction of **1** with a 1,5-cyclooctadiene(tricarboxyl)ruthenium, **6** (Scheme 2). This exchange reaction proceeds in very mild conditions (0.5 h at 50 °C). The resulting complex **5** can be chromatographed in the air to give spectrally pure samples. However, it decomposes slowly in solution, which prevented its recrystallization and microanalysis.

Both complexes undergo further rearrangements upon heating over 80 °C. The iron complex **3** gives cleanly ($\eta^5\text{-C}_7\text{H}_7$)Fe(CO)₂SnPh₃ (**7**)¹⁵ (Scheme 3). A similar transformation yielding ($\eta^5\text{-C}_7\text{H}_7$)Ru(CO)₂SnPh₃ (**8**)¹⁵ occurs to some extent with the ruthenium complex **5**; however the main product of the thermal rearrangement of **5** is a trimetallic complex **9** (Scheme 3). The

(11) Cotton, F.; Reich, C. R. *J. Am. Chem. Soc.* **1969**, *91*, 847.

(12) (a) Bennett, M. J.; Pratt, J. L.; Simpson, K. A.; LiShingMan, L. K. K.; Takats, J. *J. Am. Chem. Soc.* **1976**, *98*, 4810. (b) Salzer, A.; Egolf, T.; von Philipsborn, W. *Helv. Chim. Acta* **1982**, *65*, 1145. (c) Ball, R. G.; Edelmann, F.; Kiel, G.-Y.; Takats, J.; Drews, R. *Organometallics* **1986**, *5*, 829. (d) Edelmann, F.; Takats, J. *J. Organomet. Chem.* **1988**, *344*, 351. (e) Astley, S. T.; Takats, J. *J. Organomet. Chem.* **1989**, *363*, 167. (f) Fu, W.; McDonald, R.; Takats, J.; Bond, A. H.; Rogers, R. D. *Inorg. Chim. Acta* **1995**, *229*, 307. (g) Airolidi, M.; Beringhelli, T.; Deganello, G.; Gennaro, G.; Moret, M.; Saiano, F.; Sironi, A. *Inorg. Chim. Acta* **1995**, *229*, 461. (h) Airolidi, M.; Deganello, G.; Gennaro, G.; Moret, M.; Sironi, A. *J. Chem. Soc., Chem. Commun.* **1992**, 850. (i) Airolidi, M.; Deganello, G.; Gennaro, G.; Moret, M.; Sironi, A. *Organometallics* **1993**, *12*, 3964. (j) Wadepohl, H.; Galm, W.; Pritzkow, H. *Angew. Chem.* **1990**, *102*, 701. (k) Wadepohl, H.; Galm, W.; Wolf, A. *J. Organomet. Chem.* **1993**, *452*, 193. (l) Wadepohl, H.; Galm, W.; Pritzkow, H. *Organometallics* **1996**, *15*, 570.

(13) Gridnev, I. D.; Tok, O. L.; Gurskii, M. E.; Bubnov, Yu. N. *Chem. Eur. J.* **1996**, *2*, 1483.

(14) Gridnev, I. D.; Tok, O. L. *J. Am. Chem. Soc.* **2003**, *125*, 14700.

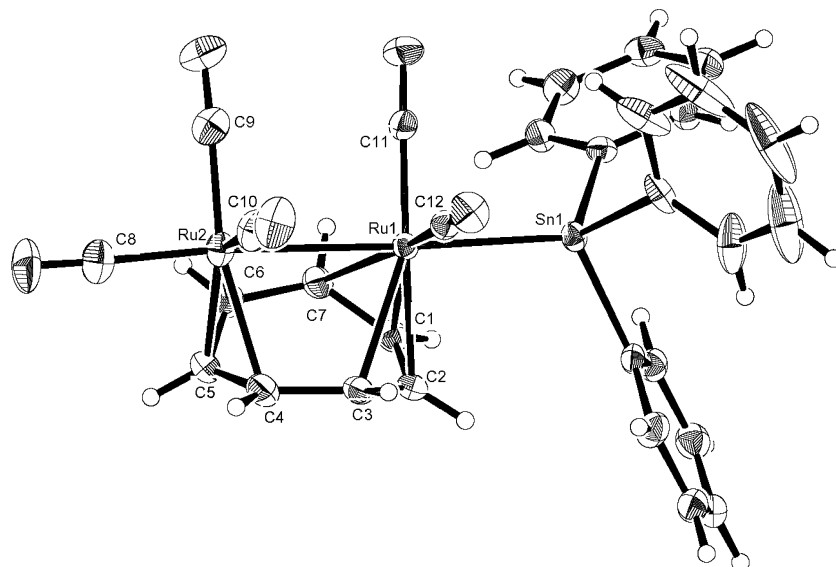
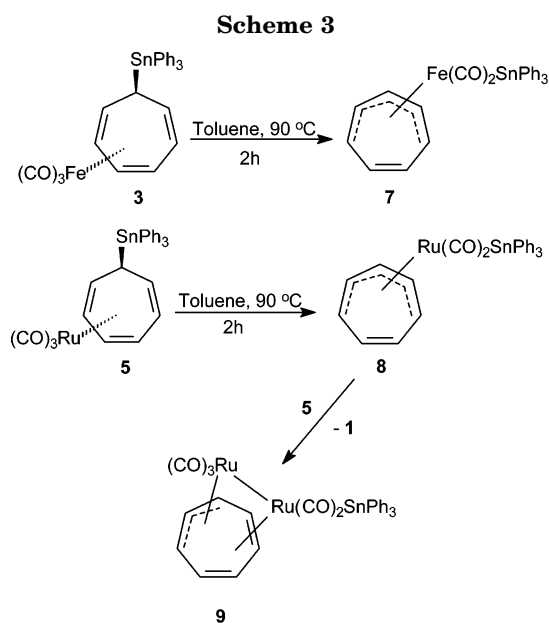


Figure 2. ORTEP diagram of complex **9** (50% thermal ellipsoids). Selected bond lengths (Å): Sn(1)–Ru(1) 2.6490(6), Ru(1)–Ru(2) 2.9060(7), Ru(1)–C(1) 2.218(5), Ru(1)–C(2) 2.214(5), Ru(1)–C(3) 2.364(6), Ru(1)–C(7) 2.332(6), Ru(1)–C(11) 1.886(6), Ru(1)–C(12) 1.894(6), Ru(2)–C(4) 2.237(6), Ru(2)–C(5) 2.171(5), Ru(2)–C(6) 2.265(6), Ru(2)–C(9) 1.920(8), Ru(2)–C(10) 1.928(7), Ru(2)–C(8) 1.909(9). Selected bond angles (deg): Sn(1)–Ru(1)–Ru(2) 177.74(2), Ru(1)–Ru(2)–C(11) 174.6(2).



complex **9** is fluxional, exhibiting only averaged signals in the ^1H and ^{13}C NMR spectra, which are only slightly broadened at $-100\text{ }^\circ\text{C}$. The structure of **9** has been determined by single-crystal X-ray analysis (Figure 2). Silicon and germanium analogues of **9** were previously prepared by the reaction of cycloheptatriene with $\{\text{Ru}(\text{MMe}_3)(\text{CO})_4\}_2$ ($\text{M} = \text{Si}, \text{Ge}$);¹⁶ in our case complex **9** is most probably formed by transfer of the irontricarbonyl group from **5** to **8** (Scheme 3).

Topology and Kinetics of the Fastest Intramolecular Rearrangements in Complexes 3 and 5. Totally 13 rearrangements are possible in either **3** or

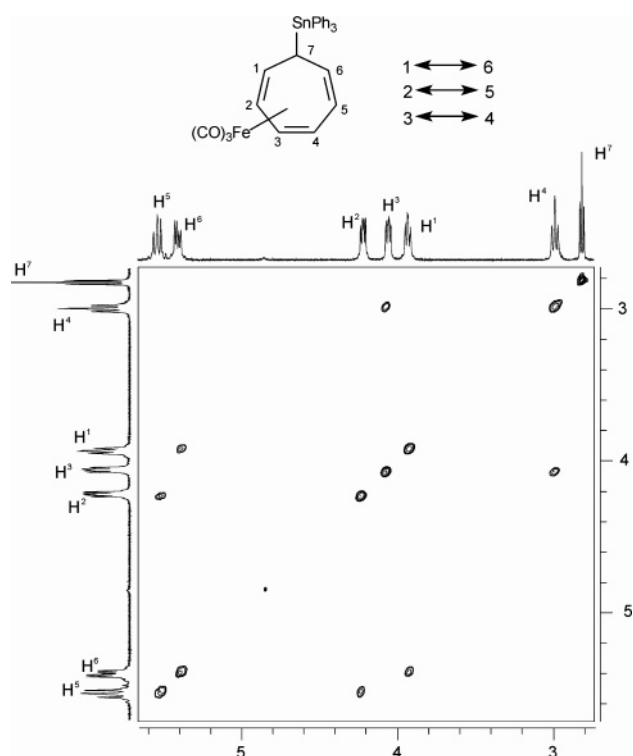


Figure 3. ^1H – ^1H 2D EXSY NMR spectrum (400 MHz, toluene- d_8 , 308 K), of compound **3**, mixing time 50 ms. Reference 1D spectra taken at 295 K are given for clarity.

5; they can be distinguished experimentally by the nature of the cross-peaks observed in the EXSY spectra (see Figures S9, S26).

Three cross-peaks observed in the phase-sensitive ^1H – ^1H or ^{13}C – ^{13}C EXSY spectra of complex **3** (e.g., Figure 3) unequivocally attest to the facile [1,3]-Fe haptotropic shift constantly occurring in this molecule. The rate of the rearrangement did not change with the concentration of the sample (in the 0.01–0.6 mol L^{-1} range) or with the variation of the inert solvent (toluene,

(15) Muhandiram, D. R.; Kiel, G.-Y.; Aarts, G. H. M.; Saez, I. M.; Reuvers, J. G. A.; Heinekey, D. M.; Graham, W. A. G.; Takats, J.; McClung, R. E. D. *Organometallics* **2002**, *21*, 2687.

(16) (a) Howard, J.; Woodward, P. *J. Chem. Soc., Dalton Trans.* **1975**, 59. (b) Brookes, A.; Knox, S. A. R.; Riera, V.; Sosinsky, B. A.; Stone, F. G. A. *J. Chem. Soc., Dalton Trans.* **1975**, 1641.

Table 1. Crystallographic Data for **3 and **9****

	3	9
chemical formula	C ₂₈ H ₂₂ FeO ₃ Sn	C ₃₀ H ₂₂ O ₅ Ru ₂ Sn
fw	581.02	783.33
solvent	hexane	hexane
cryst color, habit	yellow plate	yellow prism
cryst syst	monoclinic	monoclinic
space group	<i>P</i> 1 21/ <i>n</i> 1	<i>P</i> 1 21/ <i>a</i> 1
<i>a</i> (Å)	6.824(3)	17.043(7)
<i>b</i> (Å)	29.68(1)	14.992(6)
<i>c</i> (Å)	12.193(5)	23.022(9)
α (deg)	90	90
β (deg)	103.030(1)	109.605(2)
γ (deg)	90	90
volume (Å ³)	2406.2(1)	5541.3(39)
<i>D</i> (calcd) (g cm ⁻³)	1.604	1.878
λ (Å)	0.7107	0.7107
radiation	Mo K α	Mo K α
temperature	173.2	223.1
<i>Z</i>	4	8
cryst size (cm ³)	0.30 × 0.15 × 0.08	0.20 × 0.20 × 0.20
abs coeff (μ) (mm ⁻¹)	1.667	2.009
min./max. transmn	0.678/0.875	0.467/0.669
abs corr	multiscan	multiscan
diffractometer	Rigaku/MSC Mercury CCD	Rigaku Saturn
diffractometer	ω	ω
2 θ max (deg)	54.9	55.0
index ranges	-6 ≤ <i>h</i> ≤ 6 37 ≤ <i>k</i> ≤ 34 14 ≤ <i>l</i> ≤ 9	-22 ≤ <i>h</i> ≤ 19 -19 ≤ <i>k</i> ≤ 19 -29 ≤ <i>l</i> ≤ 26
no. reflns collected	9276	39 905
no. indep reflns	3166	8597
R(<i>F</i>) (<i>I</i> > 2 σ (<i>I</i>))	0.021	0.045
wR2 (<i>I</i> > 2 σ (<i>I</i>))	0.022	0.119
goodness of fit	1.201	0.742

benzene, chloroform, methylene chloride, cyclohexane), thus attesting to the truly intramolecular process.

Activation parameters of this rearrangement (Table 2) show that the [1,3]-Fe haptotropic shift in **3** is significantly faster than similar rearrangements in germanium derivatives¹⁷ or the parent compound.¹⁹ The rate of the [1,3]-Fe shift in **3** is comparable to that of the fastest so far known [1,3]-Fe shift in $[\eta^4\text{-}(\text{C}_6\text{H}_5\text{NCO}_2\text{-Et})\text{Fe}(\text{CO})_3]$.¹⁸

Similarly, the rutheniumtricarbyl complex **5** exhibits [1,3]-Ru haptotropic shift, a rearrangement that has not been observed previously. The activation barriers of the [1,3]-Fe and [1,3]-Ru haptotropic shifts in **3** and **5** are almost equal (Table 1), and the slightly lower rates of rearrangement in **5** compared to **3** are due to the more negative entropy of activation.

Analysis of Slower Rearrangements Taking Place in **3 and **5**.** Applying higher temperatures (308–328 K) together with relatively long mixing times (e.g., Figure 4) we detected other rearrangements occurring in **3** and **5**. To elucidate their nature, it is important to realize that the fast haptotropic shifts of the M(CO)₃ group in

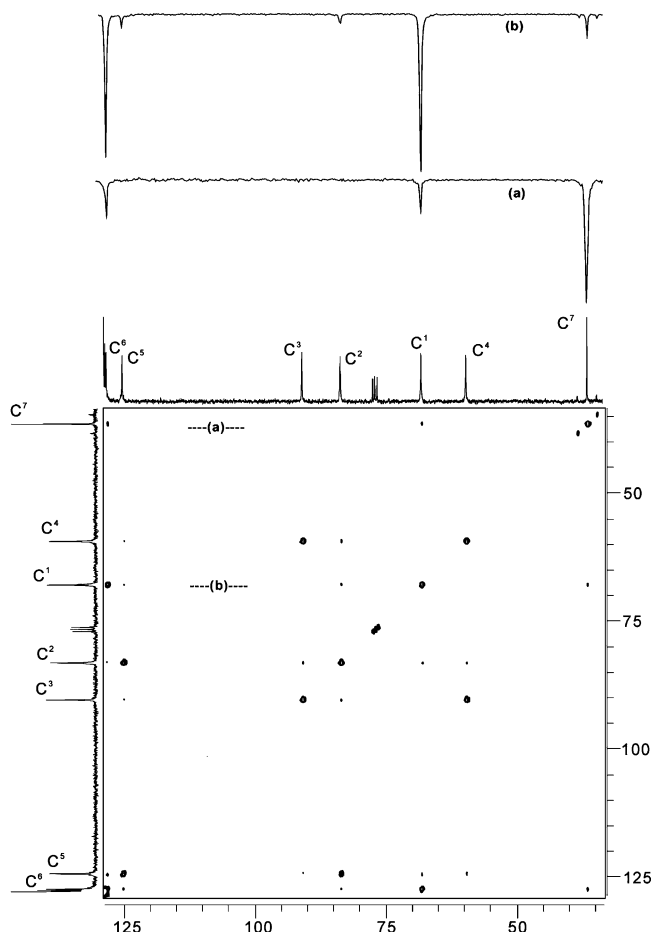


Figure 4. ¹³C–¹³C 2D EXSY NMR spectrum of complex **3** (75 MHz, toluene-*d*₈, 308 K), mixing time 80 ms, relaxation delay 3 s, number of scans 320. Traces of *F*₂ projections (a) and (b) are taken in the positions shown in the spectrum.

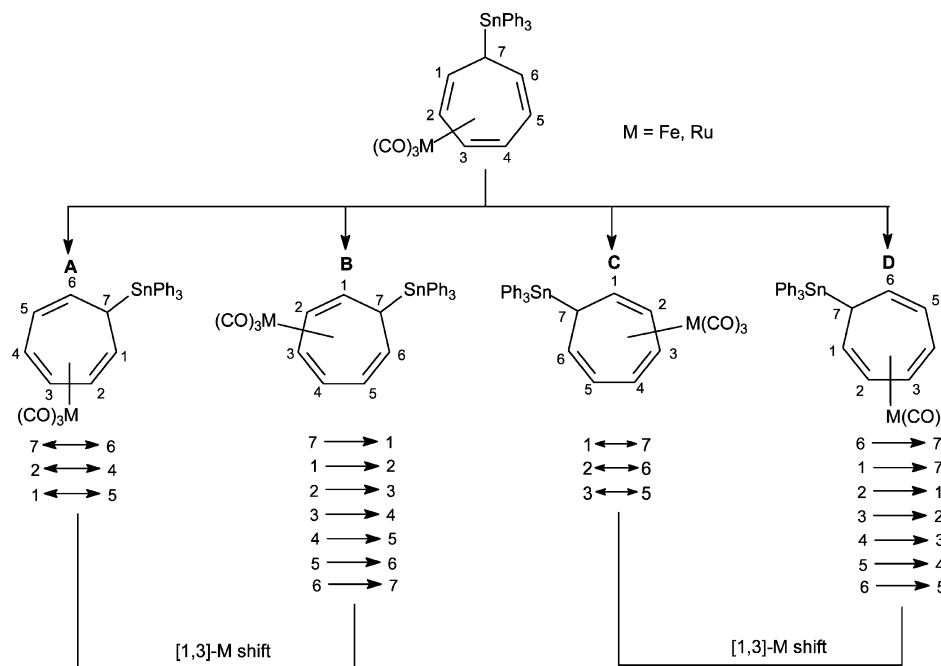
either **3** or **5** occur only in a pendant-like manner; that is, the metaltricarbyl group cannot move around the cycle due to the break of conjugation at C⁷. Therefore, any extra cross-peaks observed in the EXSY spectra at elevated temperatures attest to additional dynamic processes. From Figure 4 one can see that the carbon atom C⁷ of complex **3** (not participating in the fast exchange) has cross-peaks of comparable intensity with C¹ and C⁶. Inspecting the sets of the exchange atoms for all 13 rearrangements possible in **3** (see Scheme S9), one can conclude that all rearrangements involving β - or γ -Sn migrations can be excluded, since their occurrence must be manifested by observation of the C⁷–C², C⁷–C⁵ or C⁷–C³, C⁷–C⁴ exchanges. Therefore, only four rearrangements bringing the triphenyltin group to the

Table 2. Activation Parameters Determined in This Work

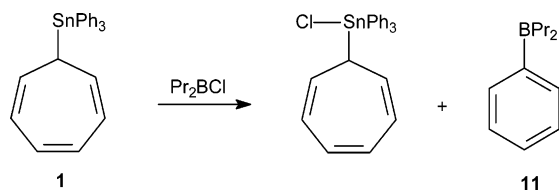
compound	reaction	nucleus	solvent	<i>T</i> , K	number of points	<i>E</i> _A ^a kJ mol ⁻¹	ln <i>A</i> ^a
3	[1,3]-Fe	¹ H	toluene- <i>d</i> ₈	268–313	9	71.4 ± 0.8	30.6 ± 0.5
		¹³ C	C ₆ D ₁₂	278–308	8	73.4 ± 5.6	31.4 ± 2.3
5	[1,3]-Ru	¹ H	toluene- <i>d</i> ₈	293–333	8	71.0 ± 4.5	28.7 ± 1.8
		¹³ C	C ₆ D ₁₂	293–318	6	70.0 ± 8.5	27.5 ± 2.8
14	[1,7]-B+[1,2]-Fe	¹ H	toluene- <i>d</i> ₈	273–313	6	70.0 ± 11	29.7 ± 5.4

^a The estimated errors were assigned by investigating all potential sources of experimental error (temperature, sample purity, chemical shift difference, number of independent measurements at each temperature, goodness of fit).²⁰ The parameters capable of causing uncertainties were manually varied, and the resulting effects of such variations on the activation parameters were summed to give the estimated errors shown in the table.

Scheme 4



Scheme 5



adjacent position (Scheme 4) can be regarded as candidates for the experimentally observed processes.

Qualitatively the set of the observed cross-peaks could be explained by any of the processes A–D followed (or preceded) by much faster [1,3]-M shift. On the other hand, the combination of several slower rearrangements cannot be excluded based only on the qualitative data. We attempted the quantitative analysis of the multisite exchange in the iron complex **3** by the ^{13}C – ^{13}C EXSY experiment carried out at 308 K (Figure 4). The use of high temperature for the experiment has been restricted by the simultaneously occurring fast migration and thermal rearrangement of **3** (vide supra). Hence, the challenge was to be able to measure the intensities of quite weak cross-peaks in the ^{13}C – ^{13}C EXSY to be certain that their intensities are not affected by NOEs and/or relayed NOEs. A sample with the maximal possible concentration (0.6 mol L^{-1}) has been used for this experiment. A series of preliminary ^1H – ^1H EXSY spectra with various mixing times (in the 10–150 ms interval) has been carried out in order to determine the maximal mixing time at that temperature not leading to the saturation of the magnetization transfer due to the fast process (80 ms). The intensity matrix obtained by the integration of the experimental phase-sensitive ^{13}C – ^{13}C spectrum is shown in the Scheme 5 together with the row of intensities of diagonal peaks obtained

in the additional experiment with mixing time 0.01 ms and the rate matrix derived using the Mestrec EXSY-Calc software. The rate of the fastest process determined in this experiment corresponds well to the value derived from the previously determined activation parameters. The mean values of the exchange rates for the slower process show some diversity. Thus, the rates for exchanges C^7 – C^1 and C^7 – C^6 are almost equal and notably higher than any other exchanges. Qualitatively this is well illustrated by two projection traces shown in the Figure 4: trace (a) shows that the intensities of the cross-peaks C^7 – C^1 and C^7 – C^6 are very similar, and trace (b) demonstrates how the C^1 – C^7 cross-peak compares to the C^1 – C^2 and C^1 – C^5 . We regard these data as evidence testifying that the diatropic migrations in **3** are not selective, viz., the triphenyltin group migrates in both directions with comparable speed. Indeed, if only one diatropic rearrangement preceded (or followed) by the [1,3]-Fe shift would occur, it should be expected that only one exchange (either C^7 – C^1 or C^7 – C^6) would be faster than the others, since this would be the only exchange repeatedly observed in both rearrangements (slow and fast+slow).

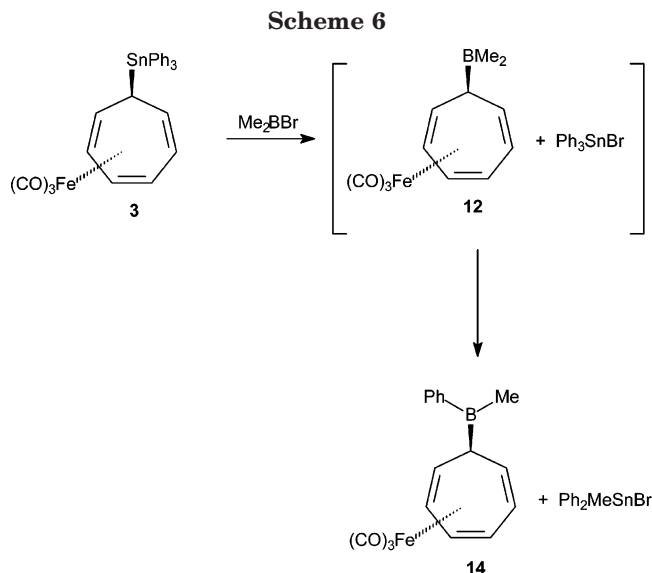
Thus, we conclude that the available data attest to two diatropic rearrangements in **3** with a different direction of tin migration. However we are unable to distinguish between several possible combinations: A+C, A+D, B+C, or B+D (Scheme 4).

Looking for the slower rearrangements in the ruthenium complex **5**, we have studied its EXSY spectra at relatively increased temperatures and longer mixing times. We were able to observe in the ^1H – ^1H EXSY spectrum taken at 323 K (see Figure S18) low-intensity cross-peaks; qualitatively the set of those was exactly the same as in the EXSY spectra of the iron complex **3**. However, the broadness of the signals due to the fast [1,3]-Ru migrations together with the limited thermal stability of the samples did not confirm this observation with the ^{13}C – ^{13}C EXSY data.

(17) LiShingMan, L. K. K.; Reuvers, J. G. A.; Takats, J.; Deganello, G. *Organometallics* **1983**, *2*, 28.

(18) Günther, H.; Wenzl, R. *Tetrahedron Lett.* **1967**, *8*, 4155.

(19) Karel, K. J.; Brookhart, M. *J. Am. Chem. Soc.* **1978**, *100*, 1619.



Reaction of the Irontricarboxyl Complex of Cycloheptatrienyl(triphenyl)tin 3 with Bromodimethylborane; Topology and Kinetics of Intramolecular Rearrangements in the Irontricarboxyl Complex of Cycloheptatrienyl(phenyl)(methyl)borane. Earlier we reported a fast diatropic [1,7]-B + [1,2]-Fe migration in the irontricarboxyl complex of cycloheptatrienyl(dipropyl)borane (**10**).¹³ Complex **3**, differing from **10** by the nature of the σ -bonded organometallic group, exhibits a different fast rearrangement, viz., the facile [1,3]-Fe shift. We therefore investigated the possibility to switch the mode of the intramolecular oscillations in the heterobimetallic complex by transmetalation reaction in solution.

Previously we have tried to prepare the cycloheptatrienylboron derivative by reacting **1** with chlorodipropylborane.²¹ However, in that case the phenyl groups exhibited much higher migration ability compared to the cycloheptatrienyl substituent, and the exchange reaction resulted in dialkylphenylboron species **11** (Scheme 5). The problem has been overcome by using trimethyl(cycloheptatrienyl)tin; however the latter compound is synthesized in a very low yield, and the transmetalation reaction is complicated by further exchange of substituents.²¹ Therefore it was tempting to try **3** in the transmetalation reaction since the electrophilic irontricarboxyl group is expected to increase the reactivity of the Sn–C(cycloheptatrienyl) bond in **3**; this effect is manifested in its very facile hydrolysis (vide supra).

Reaction of **3** with 2 equiv of bromodimethylborane proceeded smoothly and quantitatively, yielding complex **14** (Scheme 6). NMR monitoring of the reaction (e.g., Figure 6) revealed the intermediate formation of the expected complex **12** and bromotriphenyltin, which apparently react further to give **14** and bromodiphenyl(methyl)tin (Scheme 6). The boron complex **14** has been completely characterized by NMR in solution; attempts to have it in a pure form were unsuccessful so far.

Figure 7 displays the ^1H – ^1H EXSY NMR spectrum of **14** taken at 288 K. Only one rearrangement, viz., the

Intensities matrix

	c ⁷	c ⁴	c ¹	c ²	c ³	c ⁵	c ⁶
c ⁷	942		61.9				67.6
c ⁴		598		20.4	516	21.3	
c ¹	39.1		518	13.4		17.8	365
c ²		31.1	16.0	534	32.2	385	21.1
c ³		493		19.5	616	15.3	
c ⁵		22.9	18.1	411	25.1	594	27.3
c ⁶	46.6		424	15.1		28.1	594

Row of diagonal intensities in the spectrum with mixing time 0.01 ms

c ⁷	c ⁴	c ¹	c ²	c ³	c ⁵	c ⁶
1092	838	758	843	894	1049	1049

Rates matrix

	c ⁷	c ⁴	c ¹	c ²	c ³	c ⁵	c ⁶
c ⁷	-1.89	0.00	0.65	-0.01	0.00	-0.02	0.61
c ⁴	0.00	-11.46	-0.01	0.48	14.09	0.15	-0.01
c ¹	0.68	0.00	-8.85	0.20	0.00	0.13	10.11
c ²	-0.01	0.20	0.23	-9.866	0.32	10.17	0.03
c ³	0.00	15.73	-0.01	0.45	-12.09	0.24	-0.01
c ⁵	-0.03	0.42	0.19	11.85	0.03	-11.61	0.55
c ⁶	0.88	-0.01	12.03	0.29	0.00	0.45	-11.80

Rate of the fast process: $12.3 \pm 0.9 \text{ s}^{-1}$

Exchange rates

7-1	0.67	4-2	0.34
7-6	0.75	4-5	0.28
		1-2	0.22
		1-5	0.17
		2-3	0.38
		2-6	0.16
		3-5	0.14
		5-6	0.50

Figure 5. Integration matrix of the 2D ^{13}C – ^{13}C EXSY spectrum shown in Figure 4 and rates matrix obtained via matrix resolution. The auto-signal of C⁶ overlaps partially with the tin satellite of the *o*-phenyl carbon and could not be accurately integrated. It was assumed, therefore, that its intensity equals that of C⁵.

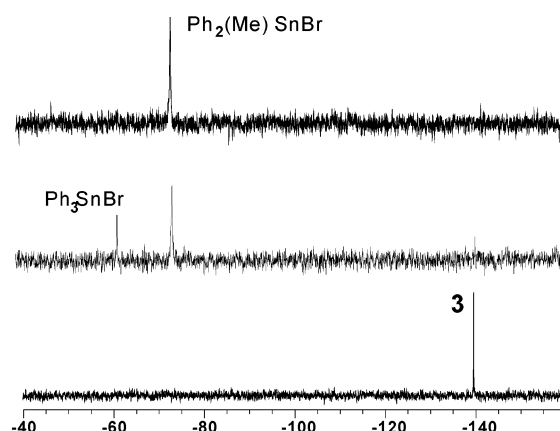


Figure 6. Monitoring of the transmetalation reaction by ^{119}Sn NMR (112 MHz, toluene- d_8 , 295 K). Bottom: the spectrum of the starting complex **3**; middle: after 2 h; top: after 4 h.

diatropic [1,7]-B + [1,2]-Fe migration, was detected in the whole range of temperatures and mixing times used for the measurements (up to 318 K and 2 s mixing time). As could be expected, the topology and the activation barrier of the fastest rearrangement in **14** (Table 2)

(20) Hayes, P. G.; Piers, W. E.; Parvez, M. *Organometallics* **2005**, *24*, 1173.

(21) Gridnev, I. D.; Tok, O. L.; Gridneva, N. A.; Bubnov, Yu. N.; Schreiner, P. R. *J. Am. Chem. Soc.* **1998**, *120*, 1034.

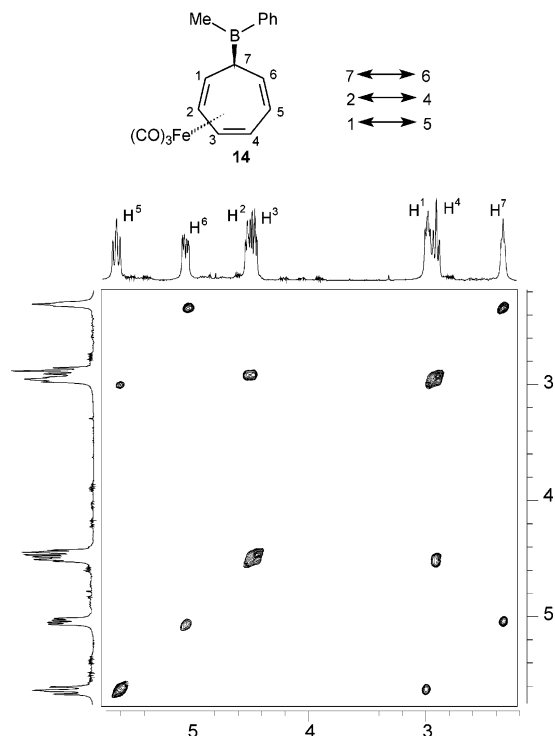


Figure 7. ^1H - ^1H 2D EXSY NMR spectrum (300 MHz, toluene- d_8 , 288 K) of compound **14**, mixing time 500 ms.

parallel the dynamic behavior of **10**; the slightly slower rate of the [1,7]-B + [1,2]-Fe diatropic migrations can be attributed to the conjugation of the unoccupied 2p-AO of boron with the phenyl ring in **14**. The same effect probably explains why we were unable to detect slower [1,3]-B and [1,3]-Fe shifts observable in **10**.

Thus, we have accomplished a chemically induced switch of the mode of metallotropic rearrangements in the fluxional molecule (Scheme 7). In the tin compound **3** fast [1,3]-Fe migrations occur in a pendant-like manner. When the tin group is exchanged to the

boryl group the character of the intramolecular oscillations becomes completely different: two organometallic groups migrate simultaneously toward each other due to a simultaneous (diatropic) [1,7]-B + [1,2]-Fe migration. This switch takes place cleanly and quantitatively at ambient temperature.

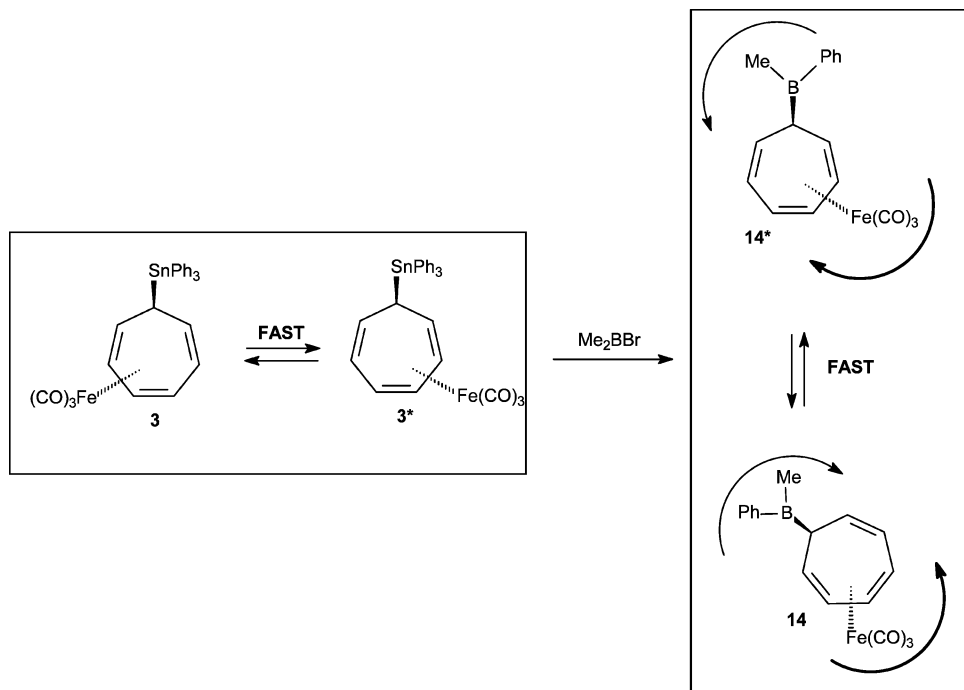
Discussion

The present work combined with the earlier results demonstrates the features of a specific type of intramolecular dynamics, viz., diatropic rearrangements in binuclear complexes. The ability of two different organometallic groups to move simultaneously within a single molecule in a highly organized manner is an interesting phenomenon both from the theoretical point of view and with respect to further implications. Although the exact mechanism of the diatropic migrations requires a separate theoretical study, it is quite clear that physically the sophisticated intramolecular reorganization occurs as a single event.

The cooperative effects between two organometallic groups are clearly seen in the rates and modes of intramolecular dynamics. The involvement of the π -system of the cycloheptatrienyl ring in the coordination with either the η^6 -bound chromiumtricarbonyl group or the η^4 -bound iron- or rutheniumtricarbonyl group effectively locks fast [1,5]-Sn sigmatropic migrations of the triphenyltin substituent. Nevertheless, the sigmatropic migration of tin is not completely suppressed in these compounds: it is observed in diatropic migrations taking place in **2**, **3**, and **5** with comparable rates and the topology is determined by the mode of coordination of the transition metal.

Moreover, from the point of view of haptotropic migrations, the [1,3]-Fe shift is significantly faster in complex **3** than in the parent compound¹⁹ or Ge- and Si-substituted derivatives.¹⁷ The fast selective diatropic migration in **10** and **14** clearly demonstrates the coop-

Scheme 7



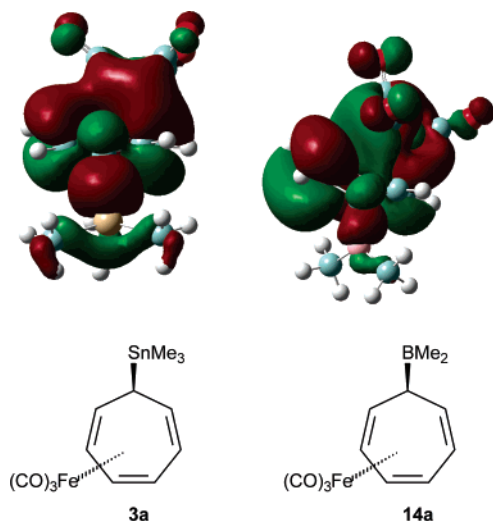


Figure 8. Molecular orbitals for the molecules **3a** and **14a** optimized at the MP2/SDD level of theory.

erative effects in the intramolecular dynamics: the [1,7]-B + [1,2]-Fe rearrangement is faster than either of the parent rearrangements.

Of interest is the observed selectivity of the rearrangements taking place in the cycloheptatrienyl bimetallic complexes. Whereas totally 13 different rearrangements are possible in compound **3**, **5**, or **14** (see Schemes S9 and S26), only three rearrangements take place in **3** or **5**, and a single rearrangement selectively occurs in **14**. Considering the molecular orbitals in boryl- and stannyl-substituted iron complexes (Figure 8), one can conclude that the symmetry of the HOMO must play an important role in determining the nature of the allowed migrations.

The HOMO of **3a** is almost perfectly symmetrical; moreover the isolobal orbital density covers the whole area involved in the [1,3]-Fe haptotropic migration. In the same area of the molecule **14a** the orbital density changes sign twice; therefore the simple [1,3]-Fe migration is disfavored in **14a** compared to **3a**. This conclusion is in good agreement with the experimental observations for **3** and **14**. Furthermore, the nonsymmetrical distribution of the orbital density with respect to the boron atom in **14a** corresponds to the exact nature of the observed diatropic rearrangement. Thus, we conclude that the selectivity of metallotropic rearrangements in heterobimetallic complexes is regulated by the symmetry of frontier orbitals, similarly to simple metallotropic rearrangements.

In complexes such as **3**, **5**, **11**, and **14** two organometallic groups are situated on opposite sides of the hydrocarbon cycle, and both are involved in the synchronous movement in a regular fashion. Therefore, physically this molecular unit would be capable of a rotational motion to a different axis or keeping the rotation of the two axes synchronized. In addition, chemically switching the mode of diatropic rearrangement, it is possible to change the direction and speed of rotation.

In conclusion, we have characterized the dynamic behavior of new heterobimetallic complexes **3** and **5**, revealed some regularities in the selectivity of diatropic migrations, and demonstrated the possibility to switch chemically the mode of intramolecular rearrangements.

Further studies along these lines using different combinations of metals and other hydrocarbon frameworks are underway in our laboratory.

Experimental Section

General Procedures. All experiments were performed under a dry argon atmosphere. The samples for NMR experiments were prepared in degassed deuterated solvents distilled prior to use over the appropriate drying agent (Na for toluene and cyclohexane, CaH₂ for CDCl₃ and CD₂Cl₂). ¹H, ¹³C, ¹¹B, and ¹¹⁹Sn NMR spectra were recorded using JEOL AL-300 and JEOL AL-400 spectrometers. Phase-sensitive ¹H and ¹³C 2D EXSY NMR spectra were acquired using a NOESYTP pulse program, slightly modified in the case of ¹³C EXSY in order to allow ¹H decoupling during acquisition. The temperature controller of the spectrometer was calibrated with the standard samples containing 4% of methanol in methanol-*d*₄ (263–293 K) and 80% of ethylene glycol in DMSO-*d*₆ from Bruker. The estimated uncertainty in temperature measurements was 0.5 K in the 263–288 and 308–333 K intervals and approximately 1 K at 288–308 K, where both methanol and ethylene glycol calibration curves become nonlinear and give somewhat contradictory results. The T₁ relaxation times have been measured for all exchanging signals in ¹H and ¹³C NMR; the relaxation times varied from 0.8 to 2.5 s. The relaxation delay was maintained to be longer than 2(T₁)_{av} (mixing time averaged for all exchanging signals).²² Mixing times were varied in the interval 20–1000 ms depending on the exchange rate at each temperature to optimize the signal-to-noise ratio. The auto- and cross-peak volumes were determined after phase and baseline correction of the two dimensions using JEOL Delta software. The signals arising from tin satellites in all cases except for the signals of H⁷ and C⁷ were integrated together with the main signals. The tin satellites of H⁷ and C⁷ (in the diagonal as well as in the cross-peaks) were integrated separately from the main signal, and their volumes were combined with those of the main peaks.

Rate constants at each temperature were derived from the experimental intensities via exchange matrix resolution approach²³ using Mestrec EXSYCalc software. For the determination of activation parameters of the fast rearrangements six values obtained from three pairs of equally populated signals arising from the same exchanging process were averaged. In the ¹³C–¹³C EXSY spectra of complex **3** the auto-signal of C⁶ overlapped partially with the tin satellite of the *o*-phenyl carbon; it was not used in the calculations. The accuracy in calculation of rate constants is determined by the accuracy of the measurements and the chemical shift differences. The signals in our experiments were well resolved; manual variation of the experimental integral values in the input matrixes according to the estimated uncertainties in the integration produced errors not larger than 10% in the averaged rate constants.

Complex 3. A Schlenk tube was filled with dry argon and charged with triphenyl(cycloheptatrienyl)tin, **1** (228 mg, 0.52 mmol), and cyclooctatetraenyl(tricarbonyl)iron, **2** (189 mg, 0.78 mmol). Dry toluene (15 mL) was added, and the reaction mixture was heated with stirring for 10 h at 100 °C. Then it was cooled, and the solvent was removed in a vacuum. The excess cyclooctatetraenyl(tricarbonyl)iron was sublimed to the upper part of the Schlenk tube (100 °C, 1 mmHg), leaving a brown oily residue at the bottom. It was collected with dry toluene. After evaporation of toluene, the residue was recrystallized from hexane to give 164 mg (54%) of pure **3** as bright yellow crystals, mp 91–92 °C. Anal. Found: C, 57.99; H, 3.85. Calcd for C₂₈H₂₂O₃SnFe: C, 57.88; H, 3.79. ¹H NMR (400 MHz,

(22) Frick, A.; Schulz, V.; Huttner, G. *Eur. J. Inorg. Chem.* **2002**, 3129.

(23) Perrin, C. L.; Dwyer, T. G. *Chem. Rev.* **1990**, *90*, 935.

toluene-*d*₈, 295 K): 2.82 (dd, 1H, H⁷, ³J_{HH} = 5.0, 5.6 Hz, ²J_{SnH} = 115, 110 Hz), 2.99 (dd, 1H, H⁴, ³J_{HH} = 7.5, 8.9 Hz, ³J_{SnH} = 22 Hz), 4.05 (ddd, 1H, H³, ³J_{HH} = 4.5, 7.5 Hz, ⁴J_{HH} = 1.2 Hz), 4.21 (ddd, 1H, H², ³J_{HH} = 4.5, 7.5 Hz, ⁴J_{HH} = 1.2 Hz, ⁴J_{SnH} = 11 Hz), 5.40 (dddd, 1H, H⁶, ³J_{HH} = 5.0, 10.4 Hz, ³J_{SnH} = 20 Hz), 5.27 (dd, 1H, H⁵, ³J_{HH} = 8.9, 10.4 Hz, ⁴J_{SnH} = 35 Hz), 7.17 (m, 9H, 6CH^m + 3CH^p arom.), 7.46 (m, 6CH^o arom.), ³J_{SnH} = 46 Hz). ¹³C NMR (100 MHz, toluene-*d*₈, 295 K): 36.65 (C⁷, ¹J_{SnC} = 270, 282 Hz), 60.04 (C⁴, ⁴J_{SnC} = 14 Hz), 68.62 (C¹, ²J_{SnC} = 22 Hz), 83.53 (C², ³J_{SnC} = 22 Hz), 90.96 (C³, ⁴J_{SnC} = 10 Hz), 126.08 (C⁵, ³J_{SnC} = 47 Hz), 128.26 (C⁶, ²J_{SnC} = 47 Hz), 128.97 (2CH^o arom., ²J_{SnC} = 35 Hz), 129.53 (CH^p arom., ⁴J_{SnC} = 12 Hz), 137.52 (2CH^m arom., ³J_{SnC} = 49 Hz), 138.53 (C–Sn arom., ¹J_{SnC} = 453, 475 Hz), 212.82 (CO). ¹¹⁹Sn NMR (112 MHz, toluene-*d*₈, 295K): –135.76. FT IR (*ν*, cm^{–1}): 1948, 1965, 1981.

Complex 5. A Schlenk tube was filled with dry argon and charged with triphenyl(cycloheptatrienyl)tin, **1** (250 mg, 0.57 mmol), and 1,5-cyclooctadienyl(tricarbonyl)ruthenium, **4** (146 mg, 0.5 mmol). Dry toluene (15 mL) was added, and the reaction mixture was heated with stirring for 1 h at 50 °C. Then it was cooled, and the solvent was removed in a vacuum. The residue was chromatographed on silica gel (eluent hexane: toluene 3:1), collecting the fraction with *R*_f 0.7. ¹H NMR (300 MHz, toluene-*d*₈, 295 K): 2.42 (ddd, 1H, H⁷, ³J_{HH} = 5.2, 5.2 Hz, ⁴J_{HH} = 1.1 Hz, ²J_{SnH} = 106, 111 Hz), 2.75 (dddd, 1H, H⁴, ³J_{HH} = 7.9, 7.9 Hz, ⁴J_{HH} = 1.0, 1.0 Hz), 3.93 (ddd, 1H, H¹, ³J_{HH} = 5.3, 7.7 Hz, ⁴J_{HH} = 1.6, 1.6 Hz, ³J_{SnH} = 14.7 Hz), 4.06 (ddd, 1H, H³, ³J_{HH} = 4.5, 7.6 Hz, ⁴J_{HH} = 1.5 Hz), 4.19 (ddd, 1H, H², ³J_{HH} = 4.4, 7.6 Hz, ⁴J_{HH} = 1.2 Hz, ⁴J_{SnH} = 7 Hz), 5.08 (dddd, 1H, H⁶, ³J_{HH} = 5.0, 10.4 Hz, ⁴J_{HH} = 1.0, 1.5 Hz, ³J_{SnH} = 19 Hz), 5.40 (dd, 1H, H⁵, ³J_{HH} = 7.9, 10.4 Hz, ⁴J_{HH} = 1.2 Hz, ⁴J_{SnH} = 27 Hz), 6.90 (m, 9H, 6CH^m + 3CH^p arom.), 7.23 (m, 6CH^o arom., ³J_{SnH} = 43 Hz). ¹³C NMR (75 MHz, toluene-*d*₈, 295 K): 33.98 (C⁷, ¹J_{SnC} = 293, 306 Hz), 51.47 (C⁴, ⁴J_{SnC} = 14 Hz), 59.00 (C¹, ²J_{SnC} = 20 Hz), 83.62 (C², ³J_{SnC} = 22 Hz), 92.11 (C³, ⁴J_{SnC} = 12 Hz), 124.09 (C⁵, ³J_{SnC} = 50 Hz), 126.57 (C⁶, ²J_{SnC} = 47 Hz), 127.54 (2CH^o arom., ²J_{SnC} = 48 Hz), 128.02 (CH^p arom., ⁴J_{SnC} = 11 Hz), 136.23 (2CH^m arom., ³J_{SnC} = 35 Hz), 137.7 (C–Sn arom., ¹J_{SnC} = 444, 468 Hz), 197.53 (CO). ¹¹⁹Sn NMR (112 MHz, toluene-*d*₈, 295 K): –140.82. FT IR (*ν*, cm^{–1}): 1987 (br), 2054.

Complex 9. A solution of (7-*exo*-triphenylstannyl)-*η*⁴-cycloheptatrienylirontricarboxyl, **3** (150 mg, 0.26 mmol), in toluene-*d*₈ (0.6 mL) was heated under argon for 1 h at 110 °C. Then the reaction mixture was cooled, the solvent was evaporated, and the residue was chromatographed on silica gel (eluent

hexane–toluene, 3:2) to yield 90 mg (60%) of the trimetallic complex **9** (*R*_f = 0.4) as bright yellow crystals together with a small amount of (*η*⁵-C₇H₇)Ru(CO)₂SnPh₃ (**8**).¹⁴ Crystals for the X-ray analysis of **9** were obtained by slow recrystallization from hexane. ¹H NMR (300 MHz, CDCl₃, 293 K): 3.96 (s, 7H, 7.29 (m, 9H), 7.42 (m, 6H). ¹³C NMR (75 MHz, toluene-*d*₈, 295 K): 64.59 (C⁷), 128.86 (3CH^p), 129.00 (6CH^m), 137.48 (6CH^o), 144.04 (3C–Sn), 196.92 (3CO), 205.05 (2CO). ¹¹⁹Sn NMR (112 MHz, toluene-*d*₈, 295 K): 31.94. FT IR (*ν*, cm^{–1}): 1942, 1975, 1996, 2073.

Complex 14. A NMR tube was filled with dry argon and charged with (7-*exo*-triphenylstannyl)-*η*⁴-cycloheptatrienylirontricarboxyl (**3**) (310 mg, 0.53 mmol). Dry toluene-*d*₈ (1 mL) was added followed by bromodimethylborane (175 mg, 1.45 mmol). The reaction progress was controlled by NMR. After 4 h at ambient temperature the sample contained only bromodiphenyl(methyl)tin (*δ*¹¹⁹Sn = –72.1) and (7-*exo*-phenyl(methyl)boryl)-*η*⁴-cycloheptatrienylirontricarboxyl, **14**: ¹H NMR (300 MHz, toluene-*d*₈, 295 K): 2.33 (dd, 1H, H⁷, ³J_{HH} = 4.2, 4.2 Hz), 2.87 (dd, 1H, H⁴, ³J_{HH} = 7.5, 7.5 Hz), 2.97 (dd, 1H, H¹, ³J_{HH} = 4.2, 6.8 Hz), 4.45 (ddd, 1H, H³, ³J_{HH} = 5.1, 10.8 Hz, ⁴J_{HH} = 1.0 Hz), 4.49 (dd, 1H, H², ³J_{HH} = 4.4, 7.6 Hz, ⁴J_{HH} = 1.2 Hz, ⁴J_{SnH} = 7 Hz), 5.02 (dd, 1H, H⁶, ³J_{HH} = 4.2, 10.4 Hz), 5.61 (ddd, 1H, H⁵, ³J_{HH} = 10.4, 10.4 Hz, ⁴J_{HH} = 1.0 Hz), 7.10–7.30 (m, 3H, 2CH^m + CH^p), 7.80 (d, 2CH^o, ³J_{HH} = 6.6 Hz). ¹³C NMR (75 MHz, toluene-*d*₈, 223 K): 13.14 (br, Me), 46.62 (br C⁷), 59.02 (C⁴), 64.19 (C¹), 86.16 (C²), 92.24 (C³), 126.83 (C⁶), 130.41 (C⁵), 129.12 (2CH), 132.43 (CH^p), 136.46 (2CH), 137.3 (br, C–B arom.), 212.55 (CO). ¹¹B NMR (MHz, toluene-*d*₈, 295 K): 74.

Acknowledgment. This work was financially supported by the COE Program “Giant molecules and complex systems” of MEXT hosted at Tohoku University, and by Grant-in-Aid for Scientific Research from MEXT (17034006). The authors thank Professor M. Kira of Tohoku University for fruitful and stimulating discussions, and Dr. C. Kabuto for X-ray structure determination. We are also grateful to the reviewers for suggesting additional useful experiments.

Supporting Information Available: Charts of all important NMR spectra, kinetic curves, analysis and classification of possible rearrangements (pdf), and detailed X-ray data (cif). This material is available free of charge via the Internet at <http://pubs.acs.org>.

OM050039I